Lanthanide(III) Complexes of a Mono(methylphosphonate) Analogue of H_4dota: The Influence of Protonation of the Phosphonate Moiety on the TSAP/SAP Isomer Ratio and the Water Exchange Rate**

Jakub Rudovský,[a] Petr Cígler,[a] Jan Kotek,[a] Petr Hermann,[a] Pavel Vojtíšek,[a] Ivan Lukeš,*[a] Joop A. Peters,*[b] Luce Vander Elst,[c] and Robert N. Muller[c]

Abstract: A monophosphonate analogue of H_4dota, 1,4,7,10-tetraazacyclododecane-4,7,10-tris(carboxymethyl)-1-methylphosphonic acid (H_5do3aP), and its complexes with lanthanides were synthesized. Multinuclear NMR studies reveal that, in aqueous solution, lanthanide(III) complexes of the ligand exhibit structures analogous to those of H_4dota complexes. Thus, the central ion is nine-coordinate, surrounded by four nitrogen atoms, three acetate and one phosphonate oxygen atoms, and one water molecule in an apical position. For complexes of H_5do3aP with Ln^{III} ions in the middle of the series, the abundance of the desired twisted square-antiprismatic (TSAP) isomer is higher than for the corresponding H_4dota complexes. The TSAP/square-antiprismatic (SAP) isomer ratio is highly sensitive to protonation of the phosphonate group: a higher abundance of the TSAP isomer was found in acidic solutions. The microscopic protonation constants of the TSAP isomers are higher than those of the SAP isomers. The presence of one water molecule in the first coordination sphere of the complexes in the pH region studied (pH 2.5–7.0) is confirmed by ^{17}O NMR spectroscopy. The results of a simultaneous fit of variable-temperature ^{17}O NMR relaxation data and ^1H NMRD profiles show that the residence time of water (τ_M) in the Gd^{III} complex is much smaller than for $[Gd(dota)(H_2O)]^-$. The exchange rate appears to be dependent on the pH of the solution. The values of τ_M are 37, 40, and 14 ns at pH 2.5, 4.7, and 7.0, respectively. These observations can be explained by an extensive second-sphere hydrogen-bonding network that varies with the state of protonation of the phosphonate moiety. Upon protonation of the complex, the second-sphere hydration probably becomes more ordered, which may result in a decrease in penetrability and an increase in τ_M. The relaxivity of the Gd^{III} complex is almost independent of the pH and is equal to $4.7\ s^{-1}\ mM^{-1}$ (20 MHz, pH 7 and 37 °C). The solid-state structure was determined for the Nd^{III} complex. It crystallizes as the TSAP isomer and the unit cell contains two independent molecules of the complex with different Nd–O(water) bond lengths of 2.499 and 2.591 Å.

Keywords: cyclen derivative · gadolinium · hydration number · MRI contrast agents · NMR spectroscopy · phosphonate complexes

Introduction

Polyazamacrocycles with coordinating pendent arms form very stable complexes with a wide range of metal ions. These ligands encapsulate metal ions in the macrocyclic cavity and the complexes often exhibit the high thermodynamic and kinetic stabilities that are essential for in vivo applications.[1] The favorable properties of these complexes

[a] J. Rudovský, P. Cígler, Dr. J. Kotek, Dr. P. Hermann, Dr. P. Vojtíšek, Prof. I. Lukeš
Department of Inorganic Chemistry, Charles University Hlavova 2030, 128 40 Prague 2 (Czech Republic)
Fax: (+420) 22-195–1253
E-mail: lukes@natur.cuni.cz

[b] Dr. J. A. Peters
Laboratory of Applied Organic Chemistry and Catalysis, Delft University of Technology
Julianalaan 136, 2628 BL Delft (The Netherlands)
Fax: (+31) 152-784-289
E-mail: j.a.peters@tnw.tudelft.nl

[c] Prof. L. Vander Elst, Prof. R. N. Muller
NMR Laboratory, Department of Organic Chemistry
University of Mons-Hainaut, Avenue du champ de Mars 24, 7000 Mons (Belgium)

[**] H_4dota = 1,4,7,10-tetraazacyclododecane-1,4,7,10-tetraacetic acid, TSAP = twisted square-antiprismatic, SAP = square-antiprismatic.

Supporting information for this article is available on the WWW under http://www.chemeurj.org/ or from the author.

 DOI: 10.1002/chem.200400367

have been exploited in several areas; for example, as contrast agents in magnetic resonance imaging (MRI)[2] or for labeling of biomolecules using metal radioisotopes for both diagnostic and therapeutic purposes.[3] The most widely studied ligand of this type, H_4dota (1,4,7,10-tetraazacyclododecane-1,4,7,10-tetraacetic acid, Scheme 1), is a prototype for the above applications.

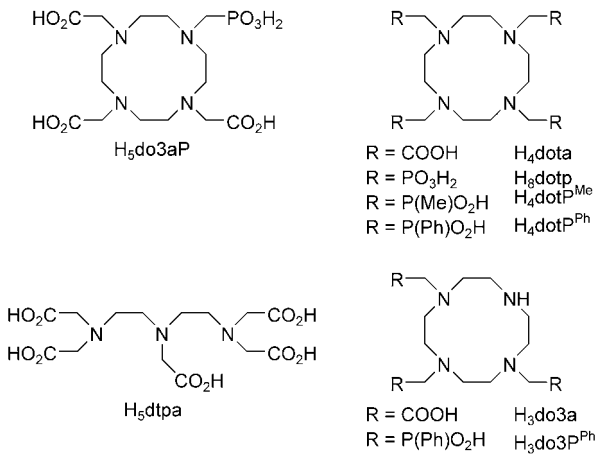

Scheme 1. Structures of ligands discussed in this paper.

In this area of chemistry, the design of better MRI contrast agents is of great importance.[4] Most of the currently approved MRI contrast agents are Gd^{III} complexes with ligands derived from acyclic H_5dtpa (diethylenetriaminepentaacetic acid, Scheme 1) or macrocyclic H_4dota. The efficiency of such contrast agents is commonly expressed as the relaxivity (r_1; the enhancement of the longitudinal water proton relaxation rate expressed in $s^{-1}\,mM^{-1}$). Relaxivity is governed by several parameters:[4]

1) The electronic relaxation time, τ_s, which is conveniently long for gadolinium(III) because of its symmetrical ^8S spin state. This correlation time remains reasonably long in complexes with a symmetric arrangement of the first coordination sphere.
2) The rotational correlation time, τ_R, which is related to the effective molecular volume of a complex (at least in the case of low-molecular-weight complexes). A high τ_R value can be achieved by covalent or noncovalent binding of the complex to (bio)macromolecules (e.g. human serum albumin; HSA).
3) The residence time, τ_M, of water molecules in the first coordination sphere of metal ions. To reach a high relaxivity, a contrast agent should exhibit a τ_M value in the optimal range (20–30 ns as predicted by theory) and a sufficiently long τ_R.[4]

All currently used MRI contrast agents have a low molecular weight although their efficiency is far from optimal because they have a too-short τ_R and/or a too-long τ_M.

Most of the recently investigated contrast agents are designed to target specific sites (e.g. cell receptors). Therefore, very efficient contrast agents giving a high contrast, even at low local concentrations, are desired. Targeting agents are often conjugates of a large bioactive addressing component and a small metal-binding moiety. Such conjugates usually have a relatively high molecular weight and, therefore, a relatively long τ_R. Hence, the relaxivity may be limited by a long τ_M of the water molecule in the Gd^{III} complex attached to the macromolecule.[4,5] Consequently, interest has been focused on the design of complexes with a smaller τ_M.

In solution, lanthanide(III) complexes of H_4dota-like ligands are typically present as a mixture of two diastereoisomers (strictly speaking as two enantiomeric pairs of diastereoisomers): the square-antiprismatic (SAP) and the twisted square-antiprismatic (TSAP) isomer (an alternative labeling with M for "major" and m for "minor" is commonly used for $[Ln(dota)(H_2O)]^-$ complexes), which are usually in fast interconversion on the NMR time scale (Figure 1).[6] It

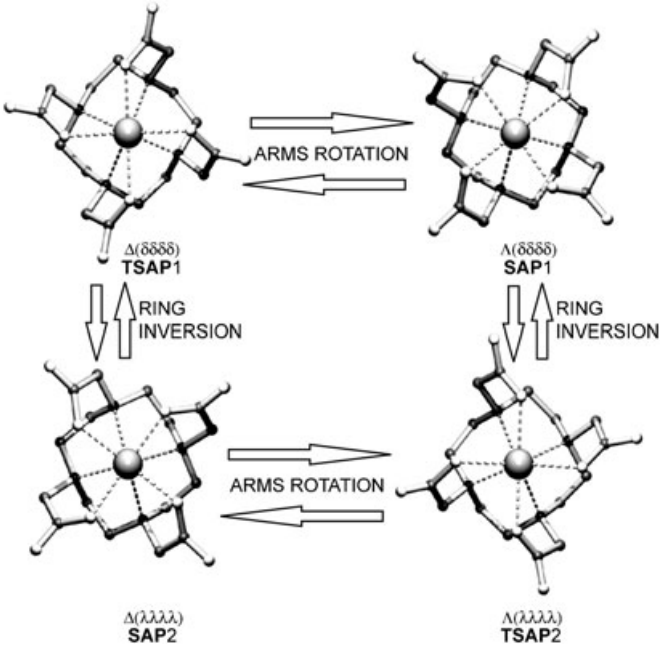

Figure 1. Summary of interconversion pathways taking place between isomers of $[Ln(dota)(H_2O)]^-$ in solution.

has been shown that these isomers display different τ_M values.[7,8] The neighborhood of the water molecule in a TSAP isomer is more sterically crowded, and therefore the water molecule exchanges 10–100 times faster than in an SAP isomer. The values of τ_M for the TSAP isomers of Gd^{III} complexes of carboxylate-bearing ligands are close to the optimal range predicted by theory.[7] Hence, Gd^{III} complexes with a higher abundance of the desired TSAP isomer should exhibit a higher relaxivity. It has also been shown that lanthanide(III) complexes of an H_4dota analogue with four phosphonic acid pendent arms are present in solution as well as in the solid state exclusively as TSAP isomers as a

consequence of the steric requirements of the phosphorus atoms.[9–12] However, no water is coordinated directly to the lanthanide(III) ions in these complexes. If a water molecule could be coordinated in similar complexes, the presence of the coordinated bulky phosphorus moiety would lead to faster water exchange. This effect has already been observed in Gd^{III} complexes of pyridine-containing macrocycles with phosphonic acid pendent arms[13] as well as upon coordination of an HPO_4^{2-} anion to Gd^{III} complexes of H_3do3a amides (H_3do3a = 1,4,7,10-tetraazacyclododecane-1,4,7-triacetic acid, Scheme 1).[14] Moreover, it is also known that the phosphonate/phosphinate complexes have a highly abundant and rather ordered second hydration sphere.[2a,10,15,16] This property has been exploited in the design of Gd^{III} complexes of tetraphosphonate H_4dota analogues, which are able to bind noncovalently to HSA.[16] These conjugates display a relatively high relaxivity because of the presence of several water molecules in the second coordination sphere of the complex moieties, with τ_M values in the nanosecond range.[16]

The present work is aimed at combining the favorable properties of complexes of H_4dota (one coordinated water molecule, high kinetic inertness, high thermodynamic stability) with those of tetraphosphorus acid analogues of H_4dota (bulkiness of the phosphorus atom and presence of only the TSAP isomer, ordering of the second hydration sphere). Therefore, we synthesized a monophosphonate analogue of H_4dota (H_5do3aP, Scheme 1) as a model compound for other ligands derived from H_4dota with one pendent arm containing a phosphorus acid moiety. The lanthanide(III) complexes were investigated by means of several NMR techniques to assess their relaxation-enhancing properties and to gain insight into the parameters that govern these relaxation processes. A preliminary conference report of this work has appeared[17] and we have recently published a complementary study on lanthanide(III) complexes of H_5dtpa analogues with a phosphonic/phosphinic acid pendent arm at the central nitrogen atom of the diethylenetriamine backbone.[18]

Results and Discussion

Synthesis of ligand and complexes: The ligand H_5do3aP was synthesized by a Mannich reaction of H_3do3a with an excess of diethylphosphite and paraformaldehyde in azeotropic aqueous HCl. The optimal temperature for the reaction is between 80 and 100 °C. Surprisingly, use of phosphonic acid instead of diethylphosphite yielded only intractable reaction mixtures. The synthesis of similar monophosphonate ligands has been mentioned briefly in a patent.[19]

Solutions of the complexes are readily obtained by mixing lanthanide(III) oxides or chlorides with solutions of a small excess of the ligand (1.1 equiv) followed by alkalization. Attempts to use a small excess of lanthanide(III) ions failed, since the excess of metal ion did not precipitate from alkaline solution and could not even be easily detected by a xylenol orange test. These phenomena may be explained by a partial formation of 2:1 Ln:L complexes, which have been detected by potentiometry during the determination of stability constants.[20] A slight excess of lanthanide(III) salts was used for the preparation of the complexes in the solid state; the excess of lanthanide ions was removed by chromatography on a silica gel column. The complexes were isolated as ammonium salts and were characterized by ESI mass spectra (see Table S1 in the Supporting Information).

Structure of $Li[Nd(Hdo3aP)(H_2O)]\cdot 11.5H_2O$: This compound crystallizes in the space group $P\bar{1}$ (no. 2) and the unit cell contains two independent complex molecules, labeled **A** and **C**. Selected bond lengths and angles for both fragments of the structure are listed in Table 1. The structure of molecule **A**, including the atom numbering scheme, is shown in Figure 2. The $(Hdo3aP)^{4-}$ ligand is coordinated to Nd^{III} by

Table 1. Selected bond lengths, angles and other geometrical parameters (in [Å] and [°]) of $Li[Nd(Hdo3aP)(H_2O)]\cdot 11.5H_2O$ (molecules **A** and **C**).

Parameter	Molecule **A**	Molecule **C**
Nd1–O1	2.499(4)	2.591(4)
Nd1–N1	2.699(5)	2.696(5)
Nd1–N4	2.736(5)	2.682(5)
Nd1–N7	2.750(5)	2.771(5)
Nd1–N10	2.676(5)	2.733(5)
Nd1–N[a]	2.715	2.720
Nd1–O11	2.431(4)	2.403(4)
Nd1–O51	2.457(4)	2.438(4)
Nd1–O71	2.435(4)	2.431(4)
Nd1–O91	2.449(4)	2.430(4)
Nd1–O[a]	2.443	2.426
Nd1–QN[b]	1.738(1)	1.746(1)
Nd1–QO[b]	0.783(1)	0.792(1)
QN–QO[b]	2.519(1)	2.535(1)
O11-Nd1-O71	142.2(1)	140.3(1)
O51-Nd1-O91	143.0(1)	143.4(1)
QN-Nd1-QO[b]	174.7(1)	174.3(1)
QN-Nd1-O1[b]	173.9(1)	171.3(1)
QO-Nd1-O1[b]	4.0(1)	4.3(1)
twist angle for pendent on N1	30.0(2)	28.9(2)
twist angle for pendent on N4	23.3(2)	23.3(2)
twist angle for pendent on N7	28.6(6)	28.1(2)
twist angle for pendent on N10	24.0(2)	23.5(2)
P1–C13	1.821(6)	1.851(6)
P1–O11	1.536(4)	1.535(4)
P1–O12	1.519(4)	1.529(4)
P1–O13	1.536(4)	1.525(4)
C15–O51	1.278(7)	1.280(7)
C15–-O52	1.235(8)	1.225(7)
O51-C15-O52	125.5(6)	125.8(6)
C17–O71	1.270(8)	1.267(8)
C17–O72	1.241(8)	1.244(7)
O71-C17-O72	125.1(6)	124.6(6)
C19–O91	1.270(7)	1.264(7)
C19–O92	1.243(7)	1.243(8)
O91-C19-O92	125.0(6)	125.5(6)
Li1–O2	1.935(12)	1.937(11)
Li1–O3	1.961(12)	1.968(12)
Li1–O13	1.905(13)	1.914(11)
Li1–O92(i)	1.926(12)	1.933(12)

[a] Mean values of Nd–N and Nd–O distances. [b] "Q" represents the centroid of the coordinated nitrogen or oxygen atoms

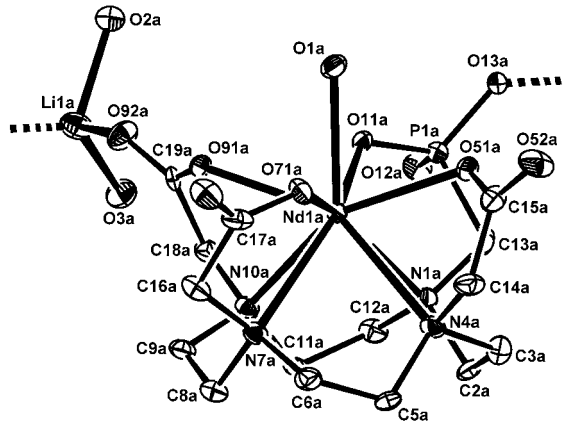

Figure 2. Molecular structure of the complex fragment in the structure of $Li[Nd(Hdo3aP)(H_2O)]\cdot 11.5\,H_2O$, with atom numbering scheme (molecule **A**).

four nitrogen atoms and three carboxylate and one phosphonate oxygen atoms. The nitrogen atoms and the oxygen atoms form N_4 and O_4 bases that are planar and virtually parallel. The angle between the planes is less than 2° in both molecules **A** and **C**. Consideration of only the carboxylate O_3 plane does not significantly change the position of the oxygen plane relative to the nitrogen plane because the mutual angle of the O_3 and O_4 planes is 0.3° for A and 1.4° for **C**, respectively. The coordinated phosphonate oxygen atom lies 0.02 Å and 0.11 Å above the O_3 plane in molecules **A** and **C**, respectively. The lanthanide ion lies between these planes, but is closer to the O_4 base (see Table 1). The twist angles of the bases around the local fourfold axis (as counted for nonequivalent pendent arms and for both the independent molecules) is between 23.3° and 30.0° (Table 1). Thus, the arrangement should be termed a twisted-square antiprism (ideal twist angle 22.5°), that is, the complex is present in the solid state as the TSAP isomer. The twist angle is almost the ideal one for the mutually opposite acetate pendent arms (on the N4 and N10 atoms) and is the same for molecules **A** and **C**. The two other pendent arms have a twist angle that is approximately 5° larger. A small difference exists in the values for the pendent phosphonate arm (30.0° for molecule **A** and 28.9° for molecule **C**). A water molecule capping the O_4 base completes the coordination sphere of Nd^{III}. The water oxygen to neodymium ion bond length, Nd–O1, is different in the two molecules (2.499(4) Å and 2.591(4) Å for molecules **A** and **C**, respectively). The hydrogen atoms of the water of hydration were not located; however, the positions found for the water oxygen atoms imply the presence of hydrogen bonds. The O1 water molecules in **A** and **C** differ in their hydrogen-bond contacts. The atom O1 in molecule **A** has a hydrogen-bond contact to phosphonate O13 (2.744(6) Å) in molecule **C**, and additional contacts to two water molecules of hydration O2w (2.809(7) Å) and O16w (3.101(7) Å). The O16w is a molecule of water with hydrogen-bond contacts to O13a of phosphonate (O13a–O16w 2.804(7) Å) and to O92a of the carboxylate (O92a–O16w 3.056(7) Å), and thus lies close to the oxygen rim of the complex (Figure 3). In solution, the presence of contacts like these would significantly influence the exchange rate of the coordinated water and also the relaxivity. The O1 atom in molecule **C** shows an

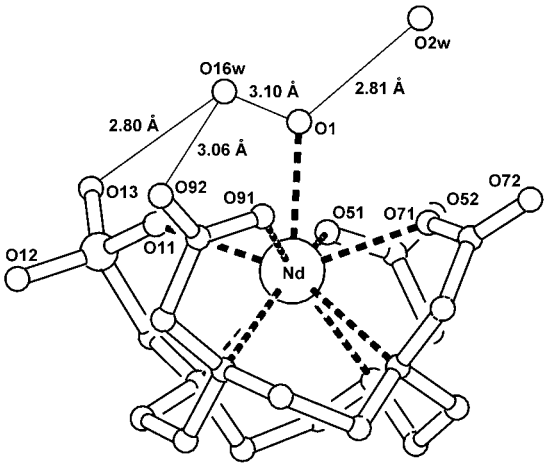

Figure 3. Hydration around the $[Nd(Hdo3aP)(H_2O)]^-$ fragment (molecule **A**).

analogous contact to the phosphonate oxygen atom O13 (2.739(6) Å) in molecule **A** and a contact to a water molecule of hydration O17w (3.128(7) Å). Thus, molecule **A**, with the shorter Nd–O1 bond length, has two hydrogen-bond contacts to hydrate water molecules, whereas molecule **C** has contact to only one hydrate water molecule. In molecule **C**, with the longer O1–Nd distance, the bond length between the central ion and the phosphonate oxygen atom is shorter than in molecule **A** (2.403(4) Å versus 2.431(4) Å, respectively) and both the distances are significantly shorter than the Nd–O(carboxylate) distances. In molecule **A**, the Nd–O(carboxylate) distances are longer than in molecule C. Accordingly, the O11-Nd-O71 angle is slightly more open in molecule **A**. All comparisons suggest that more space is available in/above the O_4 plane of molecule **A**. Thus, the differences in the Nd–O1 lengths can be ascribed to a slightly different arrangement of the ligand around the central atoms.

Comparison of our structure with that of the SAP isomer of $[Nd(dota)(H_2O)]^-$ in the solid state[21] shows that the water-to-neodymium distance in that complex (2.508 Å) is closer to that found in molecule **A**. The carboxylate oxygen–neodymium distances in the H_4dota complex (2.41–2.42 Å) are shorter than the corresponding distances in the H_5do3aP complex. In the dimeric complex $[Nd(L)]_2$ (H_3L = *N*-methylated H_3do3P^{Ph}, Scheme 1),[22] all O(P)–Nd distances are shorter (2.34–2.40 Å) than the Nd–O11 lengths observed in the H_5do3aP complex.

The lithium(I) ion is coordinated to the oxygen atom O13 of phosphonate, O92 of a carboxylate from a neighboring molecule, and two water molecules (O2 and O3). Its coordination number is 4 and the lithium subunits connect neodymium polyhedrons **A** as well as polyhedrons **C** into separate

infinite chains. Coordination of such counterions to carboxylates, phosphonates, or phosphinates is a common motif in the structures of lanthanide complexes with dota and dota-like ligands, and has been found in the structures of both SA and TSA isomers.[19,21]

Structure of lanthanide(III) complexes in solution: The chemical shifts of the NMR-active nuclei (even those which are not directly coordinated) are affected by the paramagnetic lanthanide(III) ion present in the molecule.[23] As the lanthanide-induced chemical shift (LIS) is highly directional, the structure of lanthanide(III) complexes can be partially deduced on the basis of NMR spectra. Thus, to prove and explore the ligation of lanthanide(III) ions by H_5do3aP also in solution, a multinuclear (^{1}H, ^{31}P, ^{17}O) NMR study was carried out.

^{1}H NMR spectra: The ^{1}H NMR spectra of the $[Nd(do3aP)(H_2O)]^{2-}$, $[Eu(do3aP)(H_2O)]^{2-}$, and $[Yb(do3aP)(H_2O)]^{2-}$ complexes were measured at pH 7.0 and pH 2.5 (see Figure S1 in the Supporting Information). Since the lanthanide(III) complexes of H_5do3aP have C_1 symmetry a total of 24 signals was expected to be present in the ^{1}H NMR spectra if coordination of all donor atoms was accomplished. However, the complete set of signals was observed only in the case of the Yb^{III} complex, where minimal accidental coalescence occurred. A comparison of the number and the chemical shifts of the resonances with complexes of the more symmetrical lanthanide(III) complexes of H_4dota-like ligands unambiguously confirmed that the coordination mode of the ligand in the complexes is analogous to that observed in complexes of H_4dota and H_8dotp (H_8dotp = 1,4,7,10-tetraazacyclododecane-1,4,7,10-tetrakis(methylphosphonic acid); Scheme 1).[6,12] The observed NMR signals were partially assigned by means of NOESY/EXSY experiments,[24] although a complete assignment was not possible as we were not able to obtain any 2D scalar-coupled NMR spectra. Moreover, in the ^{1}H NMR spectra of $[Eu(do3aP)(H_2O)]^{2-}$ and $[Yb(do3aP)(H_2O)]^{2-}$ complexes, the mixture of TSAP and SAP isomers is clearly visible and interconversion processes (TSAP$\rightleftharpoons$SAP) similar to those reported for H_4dota complexes[6,24] were detected in an ^{1}H EXSY spectrum of the Eu^{III} and Yb^{III} complex (see Figure S1 in the Supporting Information); in the ^{1}H NMR spectrum of $[Nd(do3aP)(H_2O)]^{2-}$ there was only one isomer (TSAP), that is, one set of signals was detected. The ^{31}P NMR spectra were also measured and found to be in agreement with the ^{1}H spectra: one ^{31}P NMR resonance was found for the Nd^{III} complex, whereas two resonances were observed for both the Eu^{III} and Yb^{III} complexes.

^{17}O LIS study: Having confirmed the octacoordination of the ligand in the Nd^{III}, Eu^{III}, and Yb^{III} complexes by ^{1}H NMR spectroscopy, it was necessary to inspect and to confirm the same situation throughout the whole lanthanide series. Unfortunately, only the above three lanthanide(III) ions allowed us to obtain reasonable resolved ^{1}H NMR spectra, thus an analysis of the chemical shifts of the water ^{17}O NMR signal in the presence of the complexes was performed to obtain information on the number of water molecules in the first coordination sphere.[23] It has been shown that the lanthanide-induced shift of a nucleus of a ligand in a lanthanide(III) complex can be given by Equation (1), where Δ is the bound shift of the nucleus under study, and δ_d is the diamagnetic contribution to its induced shift. The terms F and G are independent of the lanthanide and dependent on the nucleus in question, whereas $<S_Z>$ and C_D are independent of the ligand but dependent on the lanthanide—these values are tabulated in the literature.[23]

$$(\Delta-\delta_d)/C_D = \Delta'/C_D = (<S_Z>/C_D) \times (F+G) \qquad (1)$$

The ^{17}O NMR shifts of water in the presence of the lanthanide(III) complexes of H_5do3aP throughout the lanthanide series were measured. The exchange of water between the complex and the bulk was found to be rapid on the ^{17}O NMR time scale. The measured lanthanide(III)-induced shifts, when extrapolated to a molar ratio $[Ln^{III}]/[D_2O]$ of 1:1, represent $q\Delta'/C_D$. A plot of these extrapolated shifts versus $<S_Z>/C_D$ gave a straight line with a slope -68 (Figure 4). From Equation (1) it can been seen that the

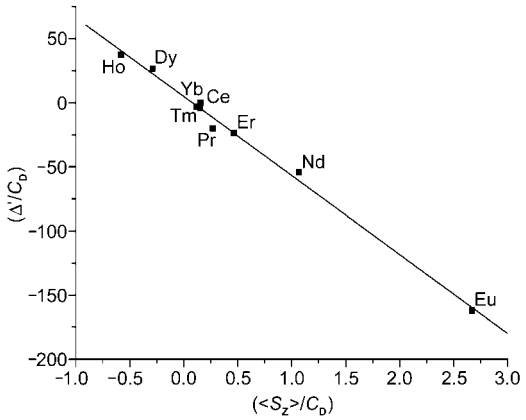

Figure 4. Linearization of ^{17}O NMR lanthanide-induced shifts of water in the presence of $[Ln(do3aP)(H_2O)]^{2-}$ (pH 7, 25 °C).

slope obtained equals qF. It has been shown previously that the parameter F falls in the range -70 ± 11 for an Ln^{III}-coordinated oxygen regardless of the nature of that oxygen. Therefore, it can be concluded that $q=1$ for the present system at pH 7, and that this value does not vary along the lanthanide series.[23]

As a complementary test the dysprosium-induced ^{17}O chemical shift (DIS)[25] in the presence of $[Dy(do3aP)(H_2O)]^{2-}$ was measured. This experiment verified that the coordination manner of the ligand remained unchanged (in the case of the Dy^{III} complex), even in acidic solutions, as only one water molecule was found at pH values 2.5, 4.5, and 7.0 at 25 °C in the first coordination sphere of the Dy^{III} ion.

^{31}P LIS study: The ^{31}P NMR spectra of the Ln^{III} complexes of H_5do3aP show a single resonance for Ce^{III}–Nd^{III} and two resonances for Sm^{III}–Yb^{III} (see Figure S2 and S3 in the Supporting Information), which confirms that mixtures of TSAP and SAP isomers are present. The exchange of the ^{31}P nuclei between the complex and the free ligand and among the complex isomers is slow on the NMR time scale. Therefore, the bound shifts could be measured directly from the spectra. The ^{31}P LIS values (for assignments of the ^{31}P NMR resonances, see below) for the SAP isomers of Sm^{III}–Yb^{III} gave a straight line when plotted according to Equation (1) (Δ'/C_D versus $<S_Z>/C_D$), thus indicating the similarity in the coordination mode of the phosphonate moiety for this series of lanthanide(III) complexes. The value for Tm^{III} lies outside the line, as is common for this ion.[23] However, a different dependence was found for the TSAP isomer. Two related data sets (Ce^{III}–Eu^{III}) and (Eu^{III}–Yb^{III}) were observed, with the Eu^{III} ion lying on the borderline. The same behavior has been observed for lanthanide(III) complexes of tetraphosphinate analogues of H_4dota (Scheme 1), which are present in aqueous solution exclusively as TSAP isomers.[10a,11] This was explained by a change in hydration of the complexes,[10a] which, however, cannot be the case for the H_5do3aP complexes (see above). Such a discrepancy between ^{17}O and ^{31}P LIS data may arise from a change in the crystal-field parameters on going from the light to the heavy lanthanide(III) ions, as was recently suggested for H_4dota and H_4dotp complexes.[26]

Dependence of the TSAP/SAP ratio on pH: Because of the presence of a readily protonatable phosphonate moiety in the lanthanide(III) complexes of our ligand, this system seems to be ideal for assessment of the impact of protonation on the properties of lanthanide(III) complexes of H_4dota-like ligands. Protonation of the phosphonate group in these complexes occurs at about pH 5.[20] However, the protonated complexes are intact at pH 2.5; acid-assisted decomplexation becomes significant only at pH < 2, where additional protonation of the carboxylate groups is expected.[20] Thus, the area we were mainly concerned about was the pH range around the pK_A value of the phosphonate moiety (2.5–7), where we have a transition from the monoprotonated species to the nonprotonated species (see Figure S4 in the Supporting Information). The ratio of TSAP/SAP isomers (and consequently the water exchange rate; see below) was a primary parameter that was expected to change upon variation of the pH. The most suitable technique to explore this was ^{31}P NMR spectroscopy, as there is a separate signal for each isomer for the various lanthanide(III) complexes.

A comparison of the intensities of these two resonances with those of TSAP and SAP in the ^{1}H NMR spectra of the Nd^{III}, Eu^{III}, and Yb^{III} complexes (see above) enabled an unambiguous assignment of the ^{31}P resonances of these complexes. However, the ^{1}H NMR spectra of the other Ln^{III} complexes were too complex to allow a determination of the TSAP/SAP ratio.

To assign the ^{31}P resonances of the latter complexes, plots of the ^{31}P NMR chemical shifts as a function of pH were made for all lanthanide complexes. In each of these ^{31}P titration curves, there was only one way in which the data points could be connected to smooth sigmoidal curves (Figure 5). Fitting of these curves with the appropriate equations afforded the pK_A values compiled in Table 2. The titration curves of the well-assigned ^{31}P spectra of the Nd^{III}, Eu^{III}, and Yb^{III} complexes showed that, for these complexes, the pK_A values of the SAP isomer are lower than those of the TSAP isomer. This can be rationalized by the relatively short Ln^{III}–P distance in the former. On the basis of these observations, the isomer with the lowest pK_A for each of the other Ln^{III} complexes was assigned to be the SAP isomer.

To exclude the influence of salts on the population of the two isomers, we compared the results obtained for samples prepared from the solid complexes with those prepared by mixing of solutions of $LnCl_3$ with the ligand followed by adjustment of the pH with KOH. Furthermore, the pH of some samples was randomly changed several times down and up by addition of concentrated acid and base solutions (see Figure 6 for the Ho complex). The same TSAP/SAP ratio was always observed. Therefore, it can be concluded that variation of the ionic strength during titrations did not influence the isomer ratio under the experimental conditions applied.

In Figure 7, the dependence of the TSAP isomer abundances (commonly used for representing the TSAP/SAP ratios) for lanthanide(III) complexes of H_3do3aP at pH 2.5, 4.8, and 7.0 are compared with that of H_4dota at pH 7. The general trend is that the TSAP abundance for the H_3do3aP complexes is significantly higher than for the corresponding H_4dota complexes, which may be ascribed to the bulkier nature of the methylphosphonate pendent arms as compared to the methylacetate arms. As a result of the increased steric strain the more compact TSAP isomers may be favored for the phosphonate compound. The relatively high abundance of TSAP in $[Gd(do3aP)(H_2O)]^{2-}$ is important in relation to its relaxivity, since it is known that the TSAP isomer usually has a τ_M value that is closer to the optimum for high relaxivity. It should be noted that the pH profiles show a monotonous decrease of the TSAP abundance upon increase of the pH for the H_4do3aP and the H_4dota complexes at pH 7, whereas for the former complexes the pH profile at pH 2.5 and 4.8 shows a local maximum at Dy^{III}.

The decrease of the TSAP/SAP ratio upon increase of the pH may be rationalized by the increased electrostatic repulsion between the phosphonate and acetate pendent arms upon ionization, which leads to a more open SAP structure and/or by an additional effect due to a change in the structure of the second hydration sphere.

It is known that phosphonic acids are able to form strong hydrogen bonds[27] and, thus, it is likely that their protonation will lead to changes in the arrangement of the hydrogen bonds between PO_3^{2-}/PO_3H^- groups and the surrounding water molecules. The water molecules involved in such a hy-

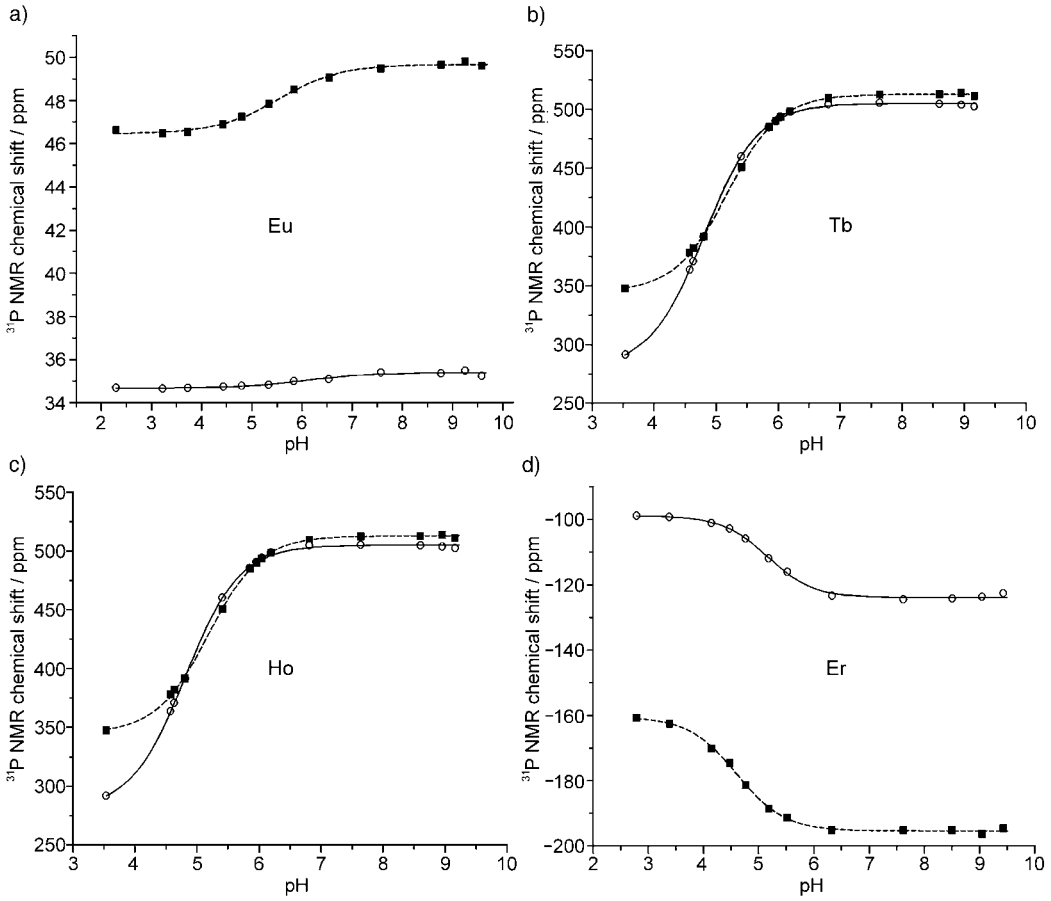

Figure 5. Dependence of δ_P of some $[Ln(H_2O)(do3aP)]^{2-}$ complexes on the pH (TSAP isomer: open circles and full line; SAP isomer: filled squares and dotted line) for Eu^{III} (a), Tb^{III} (b), Ho^{III} (c), and Er^{III} (d).

Table 2. Values of pK_A of the phosphonate group in TSAP and SAP isomers of some $[Ln(do3aP)(H_2O)]^{2-}$ complexes.

Isomer	Eu^{III}	Tb^{III}	Ho^{III}	Er^{III}
TSAP	6.0(2)[a]	5.18(1)	5.440(9)	5.16(4)
SAP	5.53(6)	4.81(1)	4.877(9)	4.60(3)

[a] The value for *TSAP*-$[Eu(do3aP)(H_2O)]^{2-}$ is a rather rough estimate due to a small difference in δ_P between the protonated and unprotonated forms.

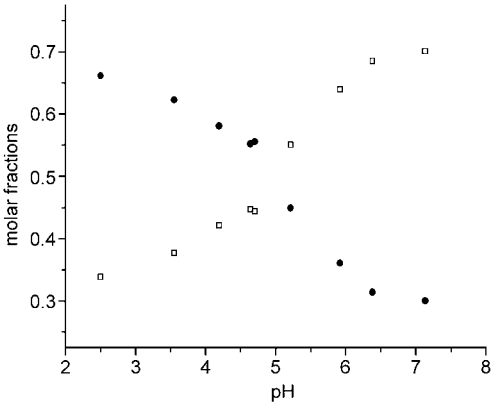

Figure 6. Dependence of molar fractions of TSAP (filled circles) and SAP (open squares) isomers on the pH for $[Ho(do3aP)(H_2O)]^{2-}$.

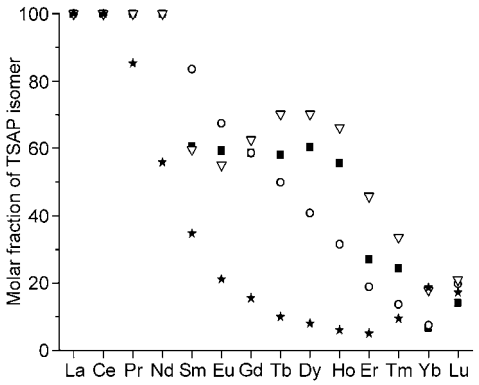

Figure 7. Dependence of the molar fraction of the TSAP isomer for Ln(III) complexes of H_5do3aP (pH 7.0: open circles; pH 4.8: filled squares; pH 2.5: open triangles) and H_4dota[6a] (pH $\approx$7: filled stars). The values for Gd^{III} complexes were interpolated from the values of the neighboring complexes.

drogen-bonding system could be either water molecules coordinated directly to the metal ion or molecules in the outer sphere. The structure of $Li[Nd(Hdo3aP)(H_2O)]\cdot 11.5\,H_2O$ presented in this paper (see above) shows both kinds of hydrogen-bond contacts. A similar situation occurs in lanthanide(III) complexes of H_8dotp, where the second hydration

sphere is highly ordered, as was found experimentally[2a,12a,16] and suggested theoretically.[28] The hydrogen-bond network in the protonated complexes of H_5do3aP would lead to a more compact arrangement of the oxygen atoms above the metal ions (involving carboxylate, phosphonate, and water oxygen atoms) and, in solution, this arrangement most likely forces the equilibrium between the two isomers in the direction of the TSAP isomer.

The pH dependence of the TSAP abundance distinguishes H_5do3aP complexes from those of H_4dota; it should be noted that the TSAP/SAP ratio for $[Eu(dota)(H_2O)]^-$ is identical at pH 1 (≈50% of $[Eu(Hdota)(H_2O)]$) and pH 7.[29]

^{17}O NMR and ^{1}H NMRD studies on the gadolinium(III) complex: A variable-temperature ^{17}O NMR study on the Gd^{III} complex was also performed at different pH values: in neutral (pH 7.0), slightly acidic (pH 4.7), and acidic (pH 2.5) solutions. As discussed above, one water molecule is coordinated at all pH values and, for Gd^{III}, the ratio of TSAP/SAP isomers is the same over the pH range under study. The TSAP/SAP ratio also appeared to be independent of the temperature between 20 and 55 °C, as was the case for the Eu^{III} complex. If the water exchange rate is governed mainly by the TSAP/SAP molar ratio, the ^{17}O profiles should be independent of the pH. However, different temperature profiles were observed (Figure 8). To get more insight into the reasons for this, ^{1}H NMRD profiles were measured at the same pH values (Figure 8). The corresponding ^{17}O NMR shift dependences and ^{1}H NMRD profiles were fitted simultaneously using a set of equations (see Supporting Information) based on the Solomon–Bloembergen–Morgan (SBM) model of paramagnetic relaxation.[2,4] This set of equations contains a huge number of parameters. Therefore, it was necessary to fix several of them. The hyperfine coupling constant of the Gd–O interaction, $A/\hbar$, was fixed at the value calculated from that of the parameter F obtained from the ^{17}O LIS measurements discussed above. The diffusion coefficient, D_{GdH}, needed for the calculation of the outer-sphere contribution to the relaxation was taken to be equal to the self-diffusion constant of water, as calculated by means of the semi-empirical relationship of Hindman.[30] The distances of gadolinium to the water O atom and H atom (R_{GdO} and R_{GdH}, respectively) were fixed at 2.5 and 3.1 Å,[31] respectively, whereas the distance of closest approach of a bulk water molecule to gadolinium (a) was taken as 3.65 Å.

From the fitting of the data for the corresponding Gd^{III} complexes of monophosphorus acid derivatives of H_5dtpa it was concluded that about two water molecules are present in the second hydration sphere of that complex.[18] In the light of the crystal structure of the Nd^{III} complex, and considering the smaller amount of space that is available above the hydrophilic oxygen atoms in the macrocyclic complexes as compared to acyclic ones, we fixed the number of second-sphere water molecules of the Gd^{III} complex of H_5do3aP, q_{ss}, to one during the fitting procedure. The residence time of this water molecule (at 298 K), τ_{mss}, was fixed, somewhat arbitrarily, to 1 ns and its activation energy, ΔH_{mss}, at 30 kJ.

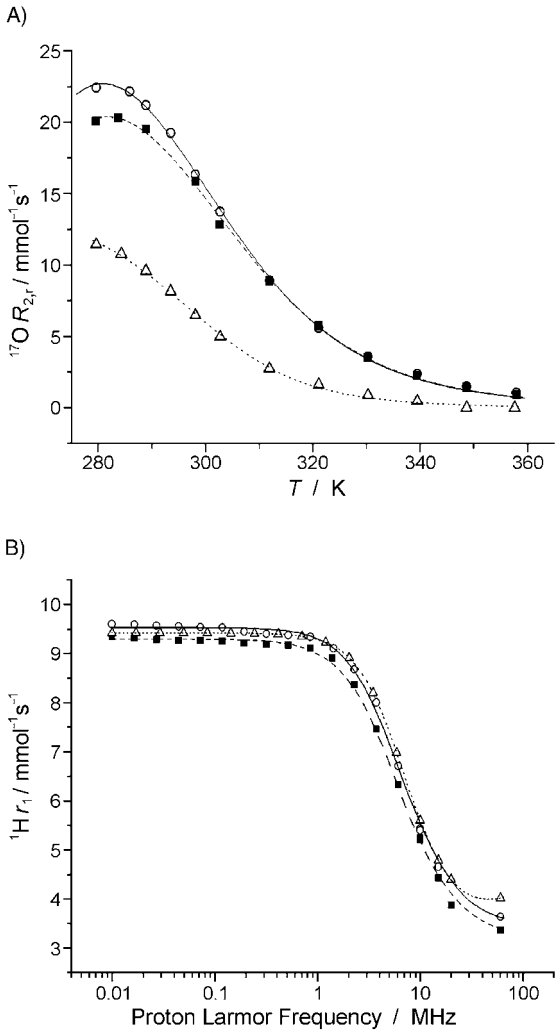

Figure 8. Temperature dependence of water ^{17}O reduced transversal relaxation time, T_{2r}, in the presence of $[Gd(do3aP)(H_2O)]^{2-}$ (A) and ^{1}H NMRD profile (B) at pH 7.0 (open triangles, dotted line), pH 4.7 (full squares, dashed line), and pH 2.5 (open circles, full line). The lines are the best fit from simultaneous fitting of ^{17}O NMR T_{2r} and ^{1}H NMRD profile.

Some other parameters defining the activation energies of correlation times (see Table 3) were fixed to the values obtained for $[Gd(dota)(H_2O)]^-$.[32] In this way, an excellent fit of the experimental data was obtained, although clearly, by fixing so many variables, only a local minimum could be identified; for example, some other reasonable fits were found when setting the first-sphere water distance longer than "usual" and the second-sphere distance shorter than "usual". The calculated curves are given in Figure 8 and the best-fit parameters are compiled in Table 3.

The obtained best-fit parameters for $[Gd(do3aP)(H_2O)]^{2-}$ at pH 7 differ from those reported for $[Gd(dota)(H_2O)]^-$ in several aspects. As we anticipated, the water residence time,

Table 3. Results from simultaneous fitting of ^{1}H NMRD and temperature dependence of ^{17}O NMR T_{2r} data in the presence of $[Gd(H_xdo3aP)(H_2O)]^{(2-x)-}$ (x = 0,1); NMRD profiles were obtained at 37 °C.

Parameter[a]	pH			H_4dota[33]
	2.5	4.7	7.0	
r_1^{310} [mmol^{-1} s^{-1}][b]	4.32	4.11	4.57	3.83
Δ^2[10^{20} s^{-2}]	0.91 ± 0.01	0.78 ± 0.02	2.07 ± 0.01	0.16
τ_M^{298} [ns]	37.0 ± 0.6	40.3 ± 0.8	14.0 ± 1	244
$\Delta H^{\neq}$ [kJ mol^{-1}]	55.8 ± 0.8	56.9 ± 0.9	76 ± 9	49.8
τ_R^{298} [ps]	70 ± 9	70 ± 9	83 ± 8	77
τ_v^{298} [ps][a]	4.6 ± 0.6	3.3 ± 0.8	3.9 ± 0.4	11
$A/\hbar$ [106 rad s^{-1}]	*−3.28*[d]	*−3.28*	*−3.28*	−3.7
R_{GdO} [Å]	*2.5*	*2.5*	*2.5*	2.38
R_{GdH} [Å]	*3.1*	*3.1*	*3.1*	–
a [Å]	*3.65*	*3.65*	*3.65*	–
$\Delta H_{ss}^{\neq}$ [kJ]	*30*	*30*	*30*	–
τ_{rss}^{298} [ps]	36 ± 4	12 ± 3	62 ± 4	–
R_{ss} [Å]	3.6 ± 0.1	3.6 ± 0.1	3.5 ± 0.1	–
τ_{mss}^{298} [ns]	*1*	*1*	*1*	–
q	*1*	*1*	*1*	*1*
q_{ss}	*1*	*1*	*1*	–

[a] Values for E_r (16.1 kJ) and E_v (1 kJ) were adjusted and fixed at H_4dota values.[32] [b] Millimolar relaxivity was measured at 37 °C and 20 MHz. [c] Italicized values were fixed during the fitting.

τ_M, for $[Gd(do3aP)(H_2O)]^{2-}$ is significantly lower (τ_M^{298} = 14 ns) than for $[Gd(dota)(H_2O)]^-$ (τ_M^{298} = 244 ns)[32] and even slightly below the optimal theoretical value. At pH 4.7 and 2.5 an increase of the water residence time was observed (40 ns and 37 ns, respectively). A similar increase in τ_M (about one order of magnitude) was also observed for $[Gd(Hdota)(H_2O)]$ upon decrease of the pH to 0–0.7, that is, after partial protonation of the coordinated carboxylates.[29] This effect was explained by a decrease of the overall negative charge of the complex.[29] Nevertheless, based on chemical reasons and the hydrogen-bond contacts found in the solid-state structure of $Li[Nd(Hdo3aP)(H_2O)]\cdot 11.5H_2O$ (see above), we want to offer an alternative explanation. We suggest that these observations may be explained by a different arrangement of the second hydration sphere of the nonprotonated and protonated species, respectively. The second hydration sphere is present in the commonly adopted model with three distinct kinds of water (i.e. one inner-sphere water molecule, some amount of the second-sphere water molecules, and the bulk water), as proposed by Merbach et al.[33] Accepting this model, two residence times representing the inner-sphere τ_M and the second-sphere τ_{mss} water exchange are commonly used and they are treated independently. The usually published water residence time τ_M corresponds to the inner-sphere water exchange. The second-sphere contribution is often neglected since, for complexes of non-phosphorus ligands, the second hydration sphere is not extensive and, moreover, τ_{mss} is considered to be much smaller (on the order of picoseconds for $[Gd(dtpa)(H_2O)]^{2-}$[34]). As for other phosphorus-containing ligands (e.g. $[Gd(Hdotp)]^{4-}$[2a]), both residence times were involved in treatment of our data.

Assuming a dissociative mechanism for the exchange of water from the first coordination sphere, an increase of the organization in the second hydration sphere will lead to an increase of the activation energy, for entropy reasons. Consequently, the residence time of water in the first coordination sphere will increase.

Support for the above-mentioned considerations comes from some examples dealing with phosphonic acid and amide derivatives of H_4dota reported in the literature. The influence of the phosphorus acid groups on the organization of the hydration is well-known in the solid state[12a,27] as well as in solution. A high hydration in solution has been observed for lanthanide(III) complexes of tetrakis(methylphosphonic/phosphinic acid) derivatives of cyclen.[2a,10,12a,16,35] As was mentioned above, the complex $[Gd(Hdotp)]^{4-}$ (the major species at neutral pH) does not contain any Gd^{III}-coordinated water; nevertheless, its second-sphere hydration gives rise to a relaxivity that is the same as for $[Gd(dota)(H_2O)]^-$.[36] The solid-state structures of lanthanide(III) complexes with H_4dota-tetraamides show a highly organized hydrogen-bond network involving the coordination of a water molecule above the O4 plane.[8,37] The τ_M^{298} in such Gd^{III} complexes is in the microsecond to millisecond range.[8,38] The dependence of the water residence time on the nature of the hydrogen-bond network has also been described for Eu^{III}–H_4dota-tetraamide complexes.[39] The most interesting contribution to the discussion seems to be Gd^{III} complexes with H_4dota monoamide derivatives bearing one or two methylphosphonates and acetate bonded to the amide nitrogen atom.[40] The charge of the complexes should be 2− or 3− depending on the protonation state of the phosphonates. The τ_M^{298} values estimated for all three complexes lie between 1.5 and 2.0 μs and are similar to the values of the amide complexes mentioned above. Therefore, an explanation of the increase of τ_M due only to the charge changes doesn't seem to be plausible.

Additional parameters such as the mean-square zero-field splitting energy (Δ^2) and the correlation time for the modulation of the zero-field splitting (ZFS) interaction (τ_v^{298}) differ slightly from those reported for $[Gd(dota)(H_2O)]^-$. These parameters change on going from pH 4.7 to 7 (Table 3). This may be due to the decrease of the symmetry upon replacement of one of the pendent acetate arms in $[Gd(dota)(H_2O)]^-$ by a methylphosphonate and its protonation/deprotonation. The other parameters of the inner sphere—the activation energy $\Delta H^{\neq}$ and rotation correlation time τ_R^{298}—are similar to those determined for $[Gd(dota)(H_2O)]^-$. The nearly optimal τ_M^{298} values found for $[Gd(do3aP)(H_2O)]^{2-}$ have a very limited effect on the relaxivity because of the low molecular weight of the complex. According to the simulation using the model utilized for data treatment, the values of the ZFS energy (Δ^2) and the correlation time (τ_v^{298}) are also slightly different from the optimal values and may reduce the overall relaxivity.

Conclusion

We have prepared a new H_4dota-like ligand with one phosphonic acid moiety. The lanthanide(III) complexes of this

ligand exhibit a similar structure to those of H_4dota (nine-coordinate, with one water in an apical position). In solution, the ratio of TSAP and SAP isomers is strongly influenced by the protonation of the phosphonate pendent arm: the desired TSAP isomer becomes more abundant in acidic solutions where the protonated form of the complexes is present. However, the TSAP/SAP isomer ratio is coincidentally independent of the pH for the Gd^{III} complex. The TSAP and SAP isomers exhibit different values of the protonation constants, with higher values for the TSAP isomer, which may be ascribed to a greater distance between the central ion and the phosphonate group. On the basis of ^{17}O NMR LIS data, we can conclude that the complexes are isostructural in solution and contain one water molecule bound directly to the central ion. From a simultaneous fitting of ^{1}H NMRD and ^{17}O NMR spectroscopic data, the water residence time, τ_M^{298}, in the Gd^{III} complex was found to be very close to the optimal value for maximal relaxivity, as predicted by theory. Such a short residence time is caused mainly by steric strain around the coordinated water molecule (induced by bulky phosphorus atom), as observed in Gd^{III} complexes of ligands where the ethylene chain is replaced by a propylene chain.[41] The relaxivity of the $[Gd(do3aP)(H_2O)]^{2-}$ complex is similar to that of $[Gd(dota)(H_2O)]^{-}$. The water residence time appears to be pH-dependent; upon acidifying the solution it becomes almost three times longer. This phenomenon may be rationalized by a decrease of the penetrability of the second hydration sphere due to a stabilization of the hydrogen-bond network in acidic solution. If this explanation of the change of τ_M^{298} with protonation is valid, the influence of the second hydration sphere on the water exchange rate should be considered when designing new high-molecular-weight contrast agents for MRI. Moreover, as there is still high demand for paramagnetic chelates with a high water exchange rate and endowed with kinetic and thermodynamic stability, the investigated ligand may become an effective contrast agent, especially upon loading to a proper high-molecular-weight carrier.

Experimental Section

H_3do3a·H_2SO_4 was a kind donation from Bracco SpA (Milano). Diethyl phosphite and H_3PO_3 were obtained from Fluka, and lanthanide(III) oxides and chlorides from Aldrich, Strem, or Alfa. Paraformaldehyde was filtered from an aged aqueous formaldehyde solution and dried in a desiccator over P_2O_5. D_2O (99.98% D) was purchased from Chemtrade (Germany). All other chemicals used were from commercial sources and were at least of analytical grade. TLC was performed on silica-coated aluminum sheets (Merck (with UV indicator) or Silufol (Kavalier, Czech Republic)) in propan-2-ol/aqueous ammonia mixtures with detection by spraying with ninhydrin or Draggendorff's reagent, or exposure to iodine vapors or UV irradiation. Elemental analyses were performed at the Institute of Macromolecular Sciences of Czech Academy of Science (Prague). ES mass spectra were recorded with a Bruker ESQUIRE 3000 with ion-trap detection in positive or negative modes.

Standard NMR measurements: Analytical and multinuclear ^{1}H, ^{31}P, ^{13}C and ^{17}O NMR studies were performed with a Varian ^{UNITY}*INOVA* 400 NMR spectrometer; (399.9 MHz (^{1}H): internal reference *t*BuOH at $\delta = 1.25$ ppm; 161.9 MHz (^{31}P): external reference 85% H_3PO_4 in D_2O at $\delta = 0$ ppm; 100.6 MHz (^{13}C): internal reference *t*BuOH at $\delta = 32.7$ ppm; 54.2 MHz (^{17}O): external reference 99.98% D_2O at $\delta = 0$ ppm). Unless otherwise stated, experiments were performed at 25 °C. The temperature was stabilized by a Highland Technology L900 TC unit and was calibrated by using MeOH and ethylene glycol. The 2D EXSY/NOESY NMR spectra were performed on a 0.1 M sample of the Yb^{III} complex (25 °C; tnnoesy pulse sequence: transmitter presaturated variation; mix = 5 ms; 32 scans; 256 increments; spectral width in both dimensions = 150000; sampling 2048×2048).

Sample preparation: NMR measurements on the lanthanide(III) complexes were performed on ~0.1 M solutions in D_2O for ^{31}P or in H_2O with ~0.2% ^{17}O enrichment for ^{17}O experiments. The pH of the samples was adjusted by addition of 1.5 M aqueous KOH or 35% HCl (Fluka, puriss.) solutions in the presence of a microscopic grain of bromocresol green indicator. For LIS measurements, the molar ratio of water per lanthanide(III) was calculated from the difference of the weights at the beginning and the end of sample preparation. The solutions were mostly prepared from the solid complexes and, in some cases (see Results and Discussion), by reaction of lanthanide(III) oxides or chlorides with 1.1 equivalents of the ligand. pH Values were determined with pHM 210 or pIONeer 10 pH-meters (both Radiometer) and combined glass microelectrodes (Radiometer or Mettler) calibrated by using commercial buffers (Radiometer). No correction was made for the deuterium isotope effect. The ionic strength of the solutions was not controlled.

Relaxometric ^{17}O and ^{1}H NMR measurements: The temperature dependence of the transversal relaxation times, T_2, of ^{17}O was measured by the Carr–Purcell–Meiboom–Gill pulse sequence; 8–10 increments on d2 exponentially sampled; at = 0.2; d1 = 0.2 ("d2" is the delay time corresponding to the echo time; "at" is acquisition time; "d1" is repetition time). These NMR spectra were recorded without frequency lock. The longitudinal relaxation times, T_1, for ^{1}H were measured by the inversion recovery pulse sequence; 12 increments on d2 exponentially sampled; at = 0.2; d1 = 0.5.

NMRD profiles: Solid samples of the ammonium salt of $[Gd(do3aP)(H_2O)]^{2-}$ were dissolved in the appropriate amount of water. The pH values were adjusted with known amounts of 10% aqueous solutions of HCl or KOH. The concentration of Gd^{III} was determined from a measurement of the bulk magnetic susceptibility.[42] NMRD profiles were measured at 37 °C at magnetic-field strengths between 4.7×10^{-4} and 0.35 T (Stelar SpinMaster FFC-2000). Additional measurements were done at 0.47 T and 1.42 T (Bruker Minispec PC 20 and mq-60, respectively) and were included in the profiles.

Data evaluation: Relaxation times T_1 and T_2 were obtained from measured data with software included in the Varian VNMR 6.1b package. Fitting of all relaxation data was done with Micromath Scientist fitting routines based on SBM equations (equations are given in the Supporting Information).[4]

Synthesis of 1,4,7,10-tetraazacyclododecane-4,7,10-tris(carboxymethyl)-1-methylphosphonic acid (H_5do3aP): H_3do3a·H_2SO_4 (5.0 g, 11.4 mmol) and $HP(O)(OEt)_2$ (5.9 mL, 45.7 mmol, 4 equiv.) were dissolved in aqueous HCl (50 mL, 1:1 v/v) and heated at a bath temperature of 85 °C. Solid $(CH_2O)_n$ (5.5 g, 183 mmol, 16 equiv) was added in small portions over 6 h and heating was continued for another 40 h. The dark brown solution obtained was filtered and the filtrate was evaporated to dryness in vacuo. The excess of HCl was removed by co-distillation with water (50 mL, three times). The residue was dissolved in water (20 mL) and the solution was poured onto a Dowex 50 column (H^+-form, 100 mL). The column was washed with water (500 mL) and the amines were eluted out with 5% aqueous ammonia (150 mL). The solvent was removed in vacuo and the residue was chromatographed on an Amberlite 50CG carboxylic resin (column bed 6×20 cm, H^+-form) with water elution. Fractions containing mainly the desired product (TLC (*i*PrOH/conc. NH_3/water 10/3/3) followed by ^{31}P NMR check) were combined, evaporated to dryness, and re-chromatographed on the same column under the same conditions. Fractions containing pure ligand (^{13}C and ^{31}P NMR check) were combined and evaporated to dryness. The residue was dissolved in water and

any colloids from the ion-exchange resins were removed with charcoal. The filtrate was evaporated to dryness and the residue was dissolved in a minimum amount of water (2 mL). The viscous solution obtained was slowly dropped into stirred absolute EtOH (500 mL). The resulting suspension was left standing overnight and the solid was filtered, washed with absolute EtOH (30 mL) and Et_2O (30 mL), and dried over P_2O_5. To remove occluded EtOH, the solid was further dried at 50 °C in vacuo (133 kPa) over P_2O_5 overnight. Finally, the solid was equilibrated in air for three days. Yield 3.0 g (55 %) of H_5do3aP·3H_2O.

R_f = 0.5 (*i*PrOH/aq. NH_3/H_2O 10/3/3), Merck sheet); ES/MS (negative mode): *m*/*z*: 439.4 [$M-H^+$]; (positive mode) *m*/*z*: 441.2 [$M+H^+$] (calcd. for $C_{15}H_{29}N_4O_9P$ 440.4); ^{1}H NMR (1 M KOD, 90 °C, *t*BuOH): δ = 3.12 (d, ^2J(P,H) = 10.1 Hz, 2H, CH_2P), 3.27 (br. m, 4H), 3.32 (br. m, 4H), 3.36 (br. m, 8H, NCH_2CH_2N), 3.52 (s, 2H, CH_2COOH), 3.68 ppm (s, 4H, CH_2COOH); ^{13}C NMR (1 M KOD, 90 °C): δ = 51.6 (2C, NCH_2CH_2N), 52.3 (1C, NCH_2CH_2N), 52.5 (1C, NCH_2CH_2N), 52.3 (d, ^1J(P,C) = 134.7 Hz, CH_2P), 57.8 (2C, CH_2COOH), 58.8 (1C, CH_2COOH), 175.4 (1C, COOH), 176.9 ppm (2C, COOH); ^{31}P NMR (1 M KOH, 90 °C): δ = 20.0 ppm (t, ^2J(P,H) = 10.1 Hz); elemental analysis calcd (%) for $C_{15}H_{29}N_4O_9P$·3H_2O (494.44): C 36.44, H 7.13, N 11.33; found: C 36.20, H 6.80, N 11.48.

Synthesis of lanthanide(III) complexes of H_5do3aP: general procedure: H_5do3aP·3H_2O (0.1 g, 0.2 mmol) was dissolved in water (2 mL) and 0.22 mmol (1.1 equiv) of the appropriate lanthanide(III) compound (oxide, chloride hydrate) was added. The suspension and/or solution was slowly neutralized by addition of an aqueous KOH solution (1.5 M) and then heated at 70 °C for at least 20 h with occasional addition of KOH solution to a final pH of about 7. The reaction mixture was filtered through a fine frit and the solvents were evaporated in vacuo. The residue was dissolved in a minimum amount of water and chromatographed on a silica column (2 × 10 cm) eluting with a mixture of *i*PrOH, concentrated aqueous NH_3, and H_2O (10/3/3). Fractions containing pure complex were collected and evaporated to dryness in vacuo. The residue was dissolved in water (0.5 mL) and any SiO_2 particles were removed by centrifugation at 4000 rpm for 10 min. The supernatant was evaporated in vacuo and the residue was dried overnight (room temperature, 133 kPa) to give the desired complexes as ammonium salts. The complexes gave correct negative ES mass spectra (Supporting Information). TLC (Merck sheets, *i*PrOH/conc. NH_3/H_2O 10/3/3): R_f of complexes ≈0.3; R_f of NH_4Cl ≈0.8; R_f of any other inorganic compound, including free lanthanide(III) salts, ≈0.0 (lanthanide(III)-containing species, complexes, and inorganic salt quench the luminescence of the sheets).

Partial assignment of the ^{1}H NMR spectrum of [Yb(do3aP)(H_2O)]$^-$ complex (see Figure S1 in the Supporting Information): TSAP isomer: δ = −39.5 (H1a), −11.9 (H1b), −3.5 (H1c), −54 (H1d), −16.1 (H2a), −2.3 (H2b), 8.5 (H2c), 40.9 (H2d), 43.8 (H3a), 20.9 (H3b), 27.8 (H3c), 6.4 (H3d), 42.2 (H4a), 61.4 (H4b), 93.7 (H4c), 115.4 (s, N-CH_2-CH_2-N, H4d), −36.0 (H5a), −27.9 (H5b), −25.7 (H5c), −13.0 (H5d), −59.0 (H6a), −50.6 (H6b), −56.5 (H6c), −56.9 ppm (s, N-CH_2-CO_2H and N-CH_2-P, H6d); SAP isomer (incomplete due to low intensity of signals): δ = 125.5 (H4), 156.4, 162.3, 176.3 ppm.

X-ray study: Diffraction-quality crystals of Li[Nd(Hdo3aP)(H_2O)]·11.5-H_2O were obtained by slow vapor diffusion of *i*PrOH into an aqueous solution of the complexes of which the pH was adjusted to about 6 using diluted aqueous LiOH solution. The selected crystal was transferred to Nujol and mounted on a glass fiber in a random orientation by means of silicon grease. Data were collected at 150(1) K (Cryostream Cooler (Oxford Cryosystem)) using a Nonius KappaCCD diffractometer and analyzed with the HKL program package.[43] The structures were solved by direct methods and refined by full-matrix least-squares techniques (SIR92[44] and SHELXL97[45]). Final geometric calculations were carried out with a recent version of the PLATON program.[46] Scattering factors for neutral atoms were included in the program SHELXL97. The hydrogens bound to carbon atoms were kept in their theoretical positions (SHELXL97); the hydrogen atoms of water molecules were not found and could not be included in the calculations. A rather high remaining peak (7.52 e Å^{-3}) was observed in the final Fourier difference map, probably due to the presence of a small crystallite on the surface of the studied crystal. This peak was not identified with any atom; no reasonable connectivity was found and thus it was suggested to be an image of the neodymium ion localized in the mentioned crystallite. Table 4 gives the pertinent crystallographic data. CCDC-227578 contains the supplementary crystallographic data for this paper. These data can be obtained free of charge from The Cambridge Crystallographic Data Centre via www.ccdc.cam.ac.uk/data_request/cif.

Table 4. Crystallographic data for Li[Nd(Hdo3aP)(H_2O)]·11.5H_2O.

Parameter	LiNd(Hdo3aP)·12.5H_2O
formula	$C_{15}H_{50}LiN_4NdO_{21.5}P$
M	812.74
T [K]	150(1)
crystal dimensions [mm]	0.4 × 0.3 × 0.2
shape and color	irregular, pale violet
crystal system	triclinic
space group	$P\bar{1}$
a [Å]	8.909(1)
b [Å]	15.938(1)
c [Å]	22.905(1)
α [°]	86.741(1)
β [°]	84.128(1)
γ [°]	84.920(1)
U [Å^3]	3218.8(1)
Z	4
ρ_{calcd} [g cm^{-3}]	1.677
λ [Å]	0.71070
μ [mm^{-1}]	1.75
F(000)	1672.0
θ range for data collection [°]	1.60–27.12
index ranges	$-10 \le h \le 11$
	$-20 \le k \le 20$
	$-29 \le l \le 29$
number of reflections measured	22519
R_σ	0.0869
number of reflections observed [$I > 2\sigma(I)$]	9338
number of independent reflections	13792
R_{int}	0.0515
coefficients in weighting scheme[a]	0.0960, 0.0000
data; restraints; parameters	13792; 0; 784
goodness-of-fit on F^2	1.046
final R_1; wR_2 indices [$I > 2\sigma(I)$][b]	0.0568; 0.1658
maximum shift [e.s.d.]	0.001
largest difference peak and hole [e Å^3]	7.52, −1.35

[a] $w = 1/[\sigma^2(F_0^2) + (A \times P)^2 + B \times P]$; where $P = (F_0^2) + 2F_c^2))/3$ (SHELXL97, ref.[45]). [b] $R_1 = \Sigma \mid F_0 - F_c \mid / \Sigma \mid F_c \mid$; $wR_2 = [\Sigma w(F_0^2) - F_c^2))^2 / \Sigma w(F_0^2))^2]^{1/2}$ (SHELXL97, ref. [45]).

Acknowledgments

We thank Bracco SpA for a kind donation of H_3do3a·H_2SO_4. Support from the Grant Agency of the Czech Republic (no. 203/02/0493 and no. 203/03/0168) and the Ministry of Education of the Czech Republic (MSM 113100001) is acknowledged. The work was done in the framework of COST D18 Action.

[1] a) M. Meyer, V. Dahaoui-Ginderey, C. Lecomte, R. Guilard, *Coord. Chem. Rev.* **1998**, *178–180*, 1313–1405; b) L. F. Lindoy, *Adv. Inorg. Chem.* **1998**, *45*, 75–125; c) K. P. Wainwright, *Coord. Chem. Rev.* **1997**, *166*, 35–90; d) S. F. Lincoln, *Coord. Chem. Rev.* **1997**, *166*, 255–289.

[2] a) M. Botta, *Eur. J. Inorg. Chem.* **2000**, 399–407; b) S. Aime, M. Botta, M. Fasano, E. Terreno, *Acc. Chem. Res.* **1999**, *32*, 941–949;

c) P. Caravan, J. J. Ellison, T. J. McMurry, R. B. Laufer, *Chem. Rev.* **1999**, *99*, 2293–2352; d) S. Aime, M. Botta, M. Fasano, E. Terreno, *Chem. Soc. Rev.* **1998**, *27*, 19–29.

[3] a) S. Liu, D. S. Edwards, *Topics in Current Chemistry*, *Vol. 222* (Ed.: W. Krause), Springer, Heidelberg, **2002**, , 259–278; b) S. Liu, D. S. Edwards, *Bioconjugate Chem.* **2001**, *12*, 7–34; c) C. J. Anderson, M. J. Welch, *Chem. Rev.* **1999**, *99*, 2219–2234; d) W. A. Volkert, T. J. Hoffmann, *Chem. Rev.* **1999**, *99*, 2269–2292; e) D. E. Reichert, J. S. Lewis, C. J. Anderson, *Coord. Chem. Rev.* **1999**, *184*, 3–66.

[4] a) *The Chemistry of Contrast Agents in Medical Magnetic Resonance Imaging* (Eds.: A. E. Merbach and É. Tóth), Wiley, Chichester (England), **2001**; b) *Topics in Current Chemistry*, *Vol. 221*, Springer Verlag, Heidelberg, **2002**.

[5] É. Tóth, D. Pubanz, S. Vauthey, L. Helm, A. E. Merbach, *Chem. Eur. J.* **1996**, *2*, 1607–1615.

[6] a) S. Aime, M. Botta, M. Fasano, M. P. M. Marques, C. F. G. C. Geraldes, D. Pubanz, A. E. Merbach, *Inorg. Chem.* **1997**, *36*, 2059–2068; b) S. Hoeft, K. Roth, *Chem. Ber.* **1993**, *126*, 869–873; c) S. Aime, L. Barbero, M. Botta, G. Ermondi, *Inorg. Chem.* **1992**, *31*, 4291–4299.

[7] a) M. Woods, Z. Kovacs, S. Zhang, A. D. Sherry, *Angew. Chem.* **2003**, *115*, 6069—6072; *Angew. Chem. Int. Ed.* **2003**, *42*, 5889–5892; b) S. Zhang, Z. Kovacs, S. Burgess, S. Aime, E. Terreno, A. D. Sherry, *Chem. Eur. J.* **2001**, *7*, 288–296; c) M. Woods, S. Aime, M. Botta, J. A. K. Howard, J. M. Moloney, M. Navet, D. Parker, M. Port, O. Rousseaux, *J. Am. Chem. Soc.* **2000**, *122*, 9781–9792.

[8] a) F. A. Dunand, R. S. Dickins, D. Parker, A. E. Merbach, *Chem. Eur. J.* **2001**, *7*, 5160–5167; b) F. A. Dunand, S. Aime, A. E. Merbach, *J. Am. Chem. Soc.* **2000**, *122*, 1506–1512; c) S. Aime, A. Barge, M. Botta, A. S. De Sousa, D. Parker, *Angew. Chem.* **1998**, *110*, 2819—2820; *Angew. Chem. Int. Ed.* **1998**, *37*, 2673–2675.

[9] I. Lukeš, J. Kotek, P. Vojtíšek, P. Hermann, *Coord. Chem. Rev.* **2001**, *216–217*, 287–312.

[10] a) S. Aime, A. S. Batsanov, M. Botta, R. S. Dickins, S. Falkner, C. E. Foster, A. Harrison, J. A. K. Howard, J. M. Moloney, T. J. Norman, D. Parker, J. A. G. Williams, *J. Chem. Soc. Dalton Trans.* **1997**, 3623–3636; b) S. Aime, A. S. Batsanov, M. Botta, J. A. K. Howard, D. Parker, K. Senanayake, J. A. G. Williams, *Inorg. Chem.* **1994**, *33*, 4696–4706.

[11] J. Rohovec, P. Vojtíšek, P. Hermann, J. Mosinger, Z. Žák, I. Lukeš, *J. Chem. Soc. Dalton Trans.* **1999**, 3585–3592.

[12] F. Avecilla, J. A. Peters, C. F. G. C. Geraldes, *Eur. J. Inorg. Chem.* **2003**, 4179–4186; b) C. F. G. C. Geraldes, A. D. Sherry, G. E. Keifer, *J. Magn. Reson.* **1992**, *97*, 290–304.

[13] a) S. Aime, E. Gianolio, D. Corpillo, C. Cavallotti, G. Palmisano, M. Sisti, G. B. Giovenzana, R. Pagliarin, *Helv. Chim. Acta* **2003**, *86*, 615–631; b) S. Aime, M. Botta, L. Frullano, S. G. Crich, G. Giovenzana, R. Pagliarin, G. Palmisano, F. R. Sirtori, M. Sisti, *J. Med. Chem.* **2000**, *43*, 4017–4024; c) S. Aime, M. Botta, S. G. Crich, G. Giovenzana, R. Pagliarin, M. Sisti, E. Terreno, *Magn. Reson. Chem.* **1998**, *36*, S200–S208.

[14] J. I. Bruce, R. S. Dickins, L. J. Govenlock, T. Gunnlaugsson, S. Lopinski, M. P. Lowe, D. Parker, R. D. Peacock, J. J. B. Perry, S. Aime, M. Botta, *J. Am. Chem. Soc.* **2000**, *122*, 9674–9684.

[15] S. Zhang, K. Wu, A. D. Sherry, *Angew. Chem.* **1999**, *111*, 3382–3384; *Angew. Chem. Int. Ed.* **1999**, *38*, 3192–3194.

[16] P. Caravan, M. T. Greenfield, X. Li, A. D. Sherry, *Inorg. Chem.* **2001**, *40*, 6580–6587.

[17] I. Lukeš, P. Cígler, J. Kotek, J. Rudovský, P. Hermann, J. Rohovec, P. Vojtíšek, *J. Inorg. Biochem.* **2001**, *86*, 68–68.

[18] J. Kotek, P. Lebdušková, P. Hermann, L. Vander Elst, R. N. Muller, T. Maschmeyer, I. Lukeš, J. A. Peters, *Chem. Eur. J.* **2003**, *9*, 5899–5915.

[19] R. Ranganathan, R. Pillai, P. C. Ratsep, R. Shulka, M. F. Tweedle, X. Zhang, WO 95/31444.

[20] P. Táborský, P. Lubal, J. Kotek, J. Rudovský, P Hermann, I. Lukeš, J. Havel, *unpublished results*.

[21] F. Benetollo, G. Bombieri, L. Calabi, S. Aime, M. Botta, *Inorg. Chem.* **2003**, *42*, 148–157.

[22] J. Rohovec, P. Vojtíšek, I. Lukeš, P. Hermann, J. Ludvík, *J. Chem. Soc. Dalton Trans.* **2000**, 141–148.

[23] J. A. Peters, J. Huskens, D. J. Raber, *Prog. NMR Spectrosc.* **1996**, *32*, 283–350.

[24] V. Jacques, J. F. Desreux, *Inorg. Chem.* **1994**, *33*, 4048–5053.

[25] M. C. Alpoin, A. M. Urbano, C. F. G. C. Geraldes, J. A. Peters, *J. Chem. Soc. Dalton Trans.* **1992**, 463–467.

[26] J. Ren, S. Zhang, A. D. Sherry, C. F. G. C. Geraldes, *Inorg. Chim. Acta* **2002**, *339*, 273–282.

[27] a) K. L. Nash, R. D. Rogers, J. Ferraro, J. Zhang, *Inorg. Chim. Acta* **1998**, *269*, 211–223; b) L. M. Shkolnikova, M. A. Porai-Koshits, *Usp. Khim.* **1990**, *59*, 1111–1143.

[28] A. Borel, L. Helm, A. E. Merbach, *Chem. Eur. J.* **2001**, *7*, 600–610.

[29] E. Szilágyi, É. Tóth, E. Brücher, A. E. Merbach, *J. Chem. Soc. Dalton Trans.* **1999**, 2481–2486.

[30] J. C. Hindman, *J. Chem. Phys.* **1974**, *60*, 4488–4496.

[31] a) A. V. Astashkin, A. M. Raitsimring, P. Caravan, *J. Phys. Chem. A* **2004**, *108*, 1990–2001; b) P. Caravan, A. V. Astashkin, A. M. Raitsimring, *Inorg. Chem.* **2003**, *42*, 3972–3974.

[32] D. H. Powell, O. M. N. Dhubhghaill, D. Pubanz, L. Helm, Y. S. Lebedev, W. Schlaepfer, A. E. Merbach, *J. Am. Chem. Soc.* **1996**, *118*, 9333–9346.

[33] É. Tóth, L. Helm, A. E. Merbach, in *The Chemistry of Contrast Agents in Medical Magnetic Resonance Imaging* (Eds.: A. E. Merbach and É. Tóth), Wiley, Chichester, England, **2001**, pp. 45–119.

[34] K. I. Hardcastle, M. Botta, M. Fasano, G. Digilio, *Eur. J. Inorg. Chem.* **2000**, 971–977.

[35] S. Aime, M. Botta, D. Parker, J. A. G. Williams, *J. Chem. Soc. Dalton Trans.* **1996**, 17–23.

[36] S. Aime, M. Botta, E. Terreno, P. L. Anelli, F. Uggeri, *Magn. Reson. Med.* **1993**, *30*, 583–591.

[37] a) D. Parker, *Chem. Soc. Rev.* **2004**, *33*, 156–165; b) D. Parker, H. Puschmann, A. S. Batsanov, K. Senanayake, *Inorg. Chem.* **2003**, *42*, 8646–8651; c) S. Aime, A. Barge, A. S. Batsanov, M. Botta, D. D. Castelli, F. Fedeli, A. Mortillaro, D. Parker, H. Puschmann, *Chem. Commun.* **2002**, 1120–1121.

[38] S. Zhang, K. Wu, A. D. Sherry, *Invest. Radiol.* **2001**, *36*, 82–86.

[39] A. Barge, M. Botta, D. Parker, H. Puschmann, *Chem. Commun.* **2003**, 1386–1387.

[40] S. Aime, M. Botta, E. Garino, S. G. Crich, G. Giovenzana, R. Pagliarin, G. Palmisano, M. Sisti, *Chem. Eur. J.* **2000**, *6*, 2609–2617.

[41] a) S. Laus, R. Ruloff, É. Tóth, A. E. Merbach, *Chem. Eur. J.* **2003**, *9*, 3555–3566; b) R. Ruloff, É. Tóth, R. Scopelliti, R. Tripier, H. Handel, A. E. Merbach, *Chem. Commun.* **2002**, 2630.

[42] D. M. Corsi, C. Platas-Iglesias, H. van Bekkum, J. A. Peters, *Magn. Reson. Chem.* **2001**, *39*, 723–726.

[43] Z. Otwinovski, W. Minor, *HKL Denzo and Scalepack Program Package* by Nonius BV, Delft, **1997**. For a reference see: Z. Otwinovski, W. Minor, *Methods Enzymol.* **1997**, *276*, 307.

[44] A. Altomare, M. C. Burla, M. Camalli, G. Cascarano, C. Giacovazzo, A. Guagliardi, G. Polidori, *J. Appl. Crystallogr.* **1994**, *27*, 435.

[45] G. M. Sheldrick, SHELXL97. Program for Crystal Structure Refinement from Diffraction Data, University of Göttingen, Germany, **1997**.

[46] A. L. Spek, PLATON - A Multipurpose Crystallographic Tool, see: http://www.cryst.chem.uu.nl/platon/

Received: April 15, 2004
Revised: November 29, 2004
Published online: January 31, 2005